Iranian Journal of Medical Physics

ijmp.mums.ac.ir

Dosimetric Comparison of Collapsed Cone Convolution/Superposition and Anisotropic Analytic Algorithms in the Presence of Exaskin Bolus in Radiotherapy

Leila Mohammadian[1], Mohsen Bakhshandeh[2,*], Elham Saeedzadeh[1], Ali Jabbari Arfaee[3]

1. Department of Medical Radiation Engineering, Science and Research Branch, Islamic Azad University, Tehran, Iran
2. Radiation Technology Department, Allied Medical Sciences Faculty, Shahid Beheshti University of Medical Sciences, Tehran, Iran
3. Medical Physics Department, Radiotherapy and Oncology Center of Shohada-e-Tajrish Hospital, Tehran, Iran

ARTICLE INFO

Article type:
Original Paper

Article history:
Received: May 27, 2020
Accepted: Oct 24, 2020

Keywords:
Radiotherapy
Algorithms
Dosimetry
Bolus

ABSTRACT

Introduction: Bolus-type materials are needed in case of superficial lesions radiotherapy. This work determined the dosimetric accuracy of two commercial treatment planning systems (TPS) for calculating photon dose distribution in the presence of eXaSkin bolus.

Material and Methods: Dose calculations were performed on collapsed cone convolution/superposition (CCC) and anisotropic analytical algorithm (AAA) using computed tomography (CT) images of heterogeneous CIRS phantom. EBT3 film was used to obtain percentage depth dose (PDD) curves and gamma index was utilized to compare the accuracy of the two algorithms. The passing rate of the global gamma index with the passing criterion of 3mm/3% as the standard criterion was considered 95% in this study.

Results: Surface dose in PDD curves increased in the presence of 0.5 cm thick eXaSkin bolus. The passing rates of gamma index with standard passing criterion between AAA algorithm and EBT3 film measurements without and with bolus were 95% and 95.5%, respectively, while they were equal to 96% and 97.5% for CCC algorithm.

Conclusion: There was a good agreement in dose calculation between AAA and CCC algorithms. Furthermore, eXaSkin bolus increased the surface dose by a factor of 25%.

►*Please cite this article as:*
Mohammadian L, Bakhshandeh M, Saeedzadeh E, Jabbari Arfaee A. Dosimetric Comparison of Collapsed Cone Convolution/Superposition and Anisotropic Analytic Algorithms in the Presence of Exaskin Bolus in Radiotherapy. Iran J Med Phys 2021; 18: 438-443. 10.22038/IJMP.2020.49078.1789.

Introduction

Radiotherapy has been established as the primary treatment option for most cancer malignancies due to its more accessible application and long-term advantages [1]. In this technique, the precision and accuracy of dose delivery during the treatment planning process are significant in treating target volume (tumor) and sparing the normal tissues [1].

In some inhomogeneous regions such as the chest wall, and head and neck, there are some hot spot areas in which surface dose decrease as much as 10% up to 10 mm depth [2, 3]. Therefore, in order to increase dose to a therapeutic level at or near the skin surface, where superficial tumor irradiation and skin involvement are indicated, bolus materials are commonly used [4].

Bolus is usually used in the form of a tissue-equivalent layer with a high atomic number, and creates better skin conformity contact set onto the patient to improve the accuracy of treatment [2, 4]. On the other hand, dose distribution would be different when the bolus is used; therefore, dosimetric accuracy should be introduced [4].

Treatment planning system (TPS) dose calculation algorithms such as AAA and CCC are different in complexity and the accuracy of dose modeling within heterogeneous media, especially in tissue boundaries and high atomic number materials [4].

Studies have shown that some dosimetric devices are used to evaluate the accuracy of TPS dose calculation, for example, thermoluminescent dosimeters (TLDs), films, and diodes [1, 5-7].

Gafchromic™ films have lots of advantages such as better spatial resolution, energy, and dose rate independence, a density close to soft tissue or water, less sensitivity to room light, and low post-irradiation growth [8-10]. Therefore, they are widely used in radiotherapy; for example, to verify TPSs, evaluate two-dimensional (2D) absorbed dose maps, and investigate dose distribution in small radiotherapy fields [11, 12]. Nowadays, Gafchromic EBT3 film (International Specialty Products, Wayne, NJ) is most

*Corresponding Author: Tel: +989123034665; Fax: +982126850560; Email: Mbakhshandeh@sbmu.ac.ir

commonly used for clinical dosimetry, due to its symmetric structure, which leads to eliminating the response dependence of the exposure direction [13], and also by laminating an active layer between two identical polyester layers which prevents the formation of Newton's Rings [1, 14].

Several studies have been performed to compare the dose accuracy of different algorithms [2, 4, 15]. In a study, Neil Richmond [4] assessed the dosimetric accuracy of Monaco and Masterplan TPS (Elekta AB, Sweden) photon dose calculation algorithms in the presence of brass mesh bolus (Whiting & Davis, Attleboro Falls, MA) using a Markus chamber. In another study, Ordonez-Sanz [16] investigated the surface dose with a 10-mm-thick Vaseline® bolus, a brass mesh, and 3 and 5 mm Superflab™ (Mick Radio-Nuclear Instruments, Mount Vernon, NY) using TLD and ionization chamber. In Zhen et al. [17] research, they compared the Eclipse Acuros XB (AXB) dose calculation with CCC and AAA for stereotactic ablative radiotherapy treatment planning of thoracic spinal metastases in IMRT and VMAT delivery techniques using EBT2 film.

To the best of our knowledge, no studies are investigating the accuracy of dose calculation by different algorithms using EBT3 films in the presence of eXaSkin bolus. Thus, this study aimed to evaluate the dosimetric accuracy of AAA and CCC photon dose calculation algorithms in the presence of eXaSkin bolus using heterogeneous CIRS phantom and EBT3 film.

Materials and Methods

Gafchromic™ EBT3 film calibration, scanning, and analysis

EBT3 film of 8 × 10 inches was used in this study. All measurements were carried out according to AAPM TG-55 reports [18]. The characteristics of this film have been described in the previous studies [1, 19].

To create a buildup region, 5 cm acrylic slabs and to produce full scattering conditions, 10 cm of the acrylic slabs were used on the top and underneath of the EBT3 films, respectively.[20]. A farmer type 30013 ionization chamber (0.6 cc, PTW, Freiburg, Germany) was used at the films' locations to verify the delivered absolute dose values.

Dose levels of 50, 100, 150, 200, 250, 300, 350, 400, 450, and 500 cGy were used to plot the calibration curve. It should be noted that for each dose level, three film pieces were exposed, and also three pieces of the same sheet were used to measure the background radiation (control). After 48 hours of irradiation, to stabilize the active layer color, the films were scanned with Microtek 9800XL scanner (Microtek Inc. Santa Fe Spring, CA) in 150-dpi spatial resolution at transmission scan mode in three colors (48 bit RGB). During the scanning process, all filters, contrast enhancers, and other factors were switched off. The images were stored in tagged image file format and image analysis was performed using ImageJ software (National Institute of Health, Bethesda, MD). Finally, net optical densities (ODs), and then the calibration curve were obtained based on the proposed method by Devic et al. [21]:

$$\Delta(net\ OD) = netOD - netOD^{control} = log\frac{PV_{unirradiated}}{PV_{irradiated}} - log\frac{PV^{control}_{unirradiated}}{PV^{control}_{irradiated}} \quad (1)$$

where $PV_{unirradiated}$ and $PV_{irradiated}$ are the "mean pixel values of the films before irradiation process" and "mean pixel values of the films after irradiation process", respectively.

eXaSkin bolus

eXaSkin is a high-density bolus with a mass density of 1.6 g/cm^3, moving the skin to the build-up region and allowing efficient surface irradiation. This bolus is made of two components, mixed to give rise to a moldable material that can be molded for 2 minutes before it hardens [15].

Treatment planning and irradiation

For treatment planning, CT (Siemens Somatom Emotion 16, Siemens, German) images of the CIRS phantom (Inc., Norfolk, VA) with 2 mm slice thickness were entered into Eclipse™ (Varian Medical Systems, Palo Alto, CA) and Isogray (Dosisoft, Cachan, France) TPS using AAA and CCC algorithms, respectively, to calculate the dose distribution. To compare the dose calculations, i.e. the accuracy of the two algorithms, two plans were performed in each TPS, with and without a 0.5 cm eXaSkin bolus to deliver 600 cGy to the reference point in the depth of 5 mm under the skin. The gantry and collimator angles were set to zero.

The EBT3 films were placed inside the CIRS phantom for dose distribution measurement. The phantom was exposed with 6 MV X-rays, 10 × 10 cm^2 field size, from a Varian Clinic 600 (Varian Medical Systems, Palo Alto, CA). The phantom was set at 100 cm source-to-surface distance. In addition, the beam central axis PDDs were measured using EBT3 film, with and without a 0.5 cm thick layer of eXaSkin bolus placed on top of the phantom (Figure 1).

Statistical analysis

Gamma evaluation is an available method to judge the agreement between treatment planning calculations and dose measurements as described by Low et al. [22]. The gamma analysis was performed using VeriSoft (PTW-Freiburg, Germany) software. A global gamma index was utilized with standard criteria of 3mm/3% (distance to agreement (DTA) = 3 mm and dose difference (DD) = 3%), and a 10% dose threshold. Also, a 95% point agreement between the TPS calculations and EBT3 measurements was considered a passing value. For each point, the gamma index (γ) was obtained using equation 1:

$$\gamma(\vec{r}_c, \vec{r}_m) = \sqrt{\frac{|\vec{r}_c, \vec{r}_m|^2}{DTA^2} + \frac{|D(\vec{r}_m)-D(\vec{r}_c)|^2}{\Delta D^2}} \quad (2)$$

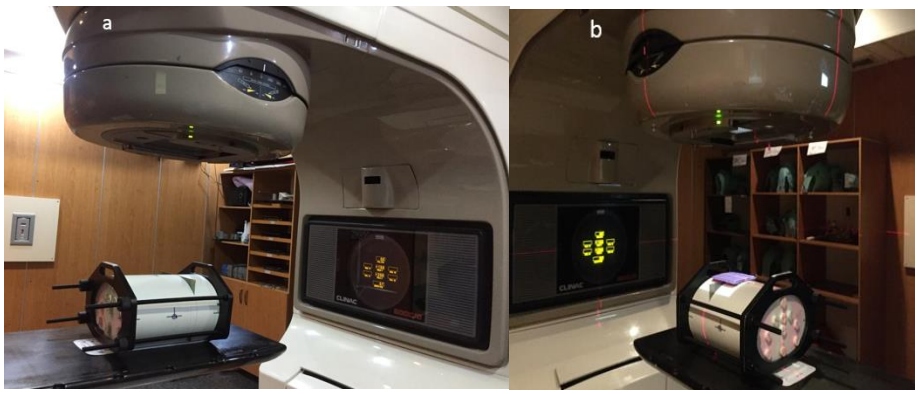

Figure 1. Radiotherapy of the heterogeneous CIRS phantom without (a) and with (b) 0.5 cm eXaSkin bolus

Where $|r_m, r_c|$ the distance between the measurement and calculation is points and $|D(r_m) - D(r_c)|$ is the dose difference between the dose distributions. Following the above equation, the failing gamma pixel was assigned a value greater than 1, and a passing pixel was assigned values between 0 and 1.

Results

EBT3 film calibration curve

The calibration curve of the film was obtained from the images of scanned films in the red channel (Figure 2). The optical density (OD)-dose curve was plotted and the equation formula was calculated using Microsoft Excel software, based on the method proposed by Devic et al. [21]. The proper fitting parameters implied an exact trinomial fitting in the dose range of 50-500 cGy.

PDD curve

The PDD curves with and without 0.5 cm eXaSkin bolus were obtained by the EBT3 film presented in Figure 3. According to this Figure, in the presence of eXaSkin bolus, the surface dose (up to 5 mm) was about 25% higher compared to the case where no bolus was present. It is clear that there is no significant difference (less than 1%) in PDD Figures in greater depths whether bolus was present or not. For further clarification, the quantitative values of the first 2 cm of Figure 3 have been presented in table 1.

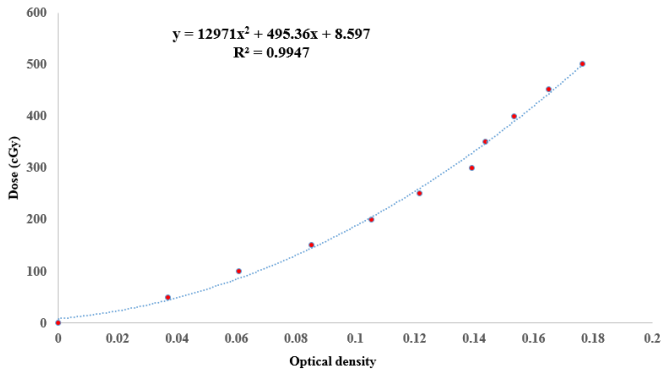

Figure 2. The film calibration curve in the red channel.

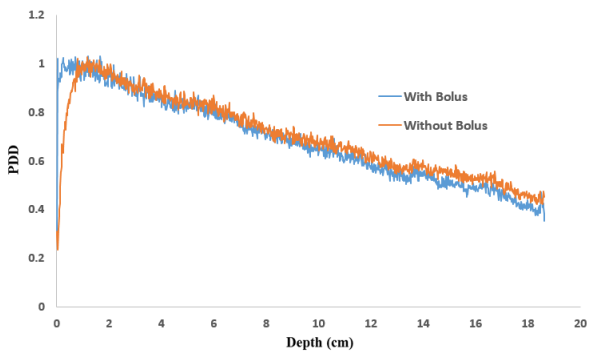

Figure 3. PDD curves obtained by EBT3 film with and without eXaSkin bolus.

Table 1. Sample data from film measurements of up to 2 cm depth.

Depth (cm)	Without bolus	With bolus	Depth (cm)	Without bolus	With bolus
0	0.3	0.3	1.1	0.99	0.95
0.05	0.23	0.89	1.15	1.01	0.98
0.1	0.4	0.92	1.2	1	1.03
0.15	0.56	0.94	1.25	1.01	0.99
0.2	0.67	0.99	1.3	1	0.99
0.25	0.65	1	1.35	0.99	0.98
0.3	0.73	0.99	1.4	1	0.98
0.35	0.74	0.98	1.45	0.98	0.99
0.4	0.8	0.97	1.5	0.99	0.99
0.45	0.85	0.98	1.55	0.98	0.95
0.5	0.84	0.95	1.6	0.97	0.93
0.55	0.89	1.01	1.65	0.95	1.03
0.6	0.91	1	1.71	0.97	1
0.66	0.93	0.99	1.76	0.95	0.95
0.71	0.92	1.02	1.81	0.98	0.95
0.81	0.94	0.98	1.84	0.93	0.91
0.84	0.96	1.01	1.91	0.98	0.92
0.91	0.98	0.93	1.94	0.98	0.9
0.94	0.95	0.99	1.98	0.97	0.95
1.01	0.97	1	2	0.96	0.94

Gamma index value

The dose distributions in the slice of CIRS phantom obtained from the film dosimetry along the central beam axis were compared with the outputs of AAA and CCC algorithms through gamma analysis.

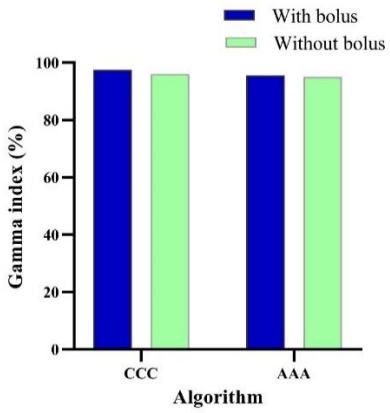

Figure 4. Comparison of gamma analysis between film dosimetry, CCC, and AAA algorithms with and without bolus.

Figure 4 presents the global gamma indices of AAA and CCC (with and without bolus) regarding the film dosimetry. The passing rates for both AAA and CCC were higher than 95% with 3mm/3% criteria (standard criteria in this study) with and without bolus. This value was equal to 95.5% and 95% for AAA with and without bolus, respectively, and it was 97.5% and 96% for CCC algorithm.

Discussion

High-quality treatment plans rely upon accurate dose calculations. A 1% improvement in accuracy results in a 2% increase in the cure rate for early-stage tumors, and a 5% change in dose, may result in a 20 to 30% change in the complication rates of normal tissues [17].

TLDs, films, and diodes are types of dosimetry tools investigating the dose accuracy in radiotherapy [1, 5, 6]. In the current study, the dosimetric accuracy of two radiotherapy systems using AAA and CCC algorithms was assessed in the presence of eXaSkin bolus.

Although high atomic number bolus materials cause a few artifacts in CT images, they can improve the conformity in the inhomogeneous regions compared to tissue-equivalent bolus [23].

In this study, the dose accuracy was obtained by Gafchromic EBT3 film, and a heterogeneous CIRS phantom, for better investigation of the algorithms. EBT3 film is one of the dosimetric tools that has lots of advantages, including tissue equivalence, high-resolution, and time and cost-saving; thus, they are used widely in radiotherapy techniques [24, 25].

Regarding the PDD curves in Figure 3, the dose was increased by about 25% in the surface region when the bolus was used. In addition, the variation of dose (with and without bolus) in depths greater than d_{max} was less than 1%. Manger et al. [23] reported that brass mesh bolus could increase the superficial dose for chest wall tangent photon radiotherapy by 35%. Also, the dose at depth when using brass mesh bolus is comparable to that measured with no bolus. Healy et al. [2] showed that a 2-mm-thick of brass mesh as a bolus could increase the surface doses between 81% and 122% of the prescribed dose in patients receiving post-mastectomy chest wall radiotherapy. In the Ordonez-Sanz study [16], they announced that 3 mm of brass mesh bolus causes 0.7% dose changes for depths greater than d_{max} and conforms superiorly to skin surfaces.

According to Figure 4, the accuracy of the AAA and CCC algorithms in the heterogeneous CIRS phantom is within standard passing criterion (3mm/3%) with and without eXaSkin bolus. Our results show that the two TPS algorithms' calculations have a good agreement with EBT3 film measurements. The decreased passing rate of gamma index (less than 100%) can be due to the lack of insufficient precision of the treatment setup, a calibration curve of film, inaccurate registration of the TPS plan, and uncertainty of the scanner reproducibility.

The gamma index passing rate was higher in the presence of 0.5 cm eXaSkin in both algorithms. The reason may be the high conformity of dose distribution in the presence of the bolus. In a study by Firouzjah et al. [12], the dose accuracy of TPS was investigated by EBT3 film and Delta4 phantom in two different points of a heterogeneous chest phantom. They showed that the mean gamma index is higher in the high conformity point.

Also, the gamma index value in the standard criterion was slightly higher in CCC compared to AAA algorithm with and without bolus. Hasenbalg et al. [26] studied the differences between CCC, AAA, and a Monte Carlo program dose distribution. Five inhomogeneous clinical cases, three lungs, and two breast cases were assessed. They expressed that the CCC algorithm calculation was better than AAA when compared to a Monte Carlo program, but AAA is used as a standard option in the clinic due to its short computation times. In another study, Aarup et al. [27] reported that AAA and CCC algorithms appeared to be alternatives and have a good agreement with Monte Carlo calculation regarding lung tumor coverage in stereotactic body radiotherapy conditions. Our findings have a good agreement with the studies mentioned above.

Future research suggests that more investigations should be conducted in the other heterogeneous organs like head and neck in the presence of eXaSkin bolus using various algorithms.

Conclusion

In the current study, the dosimetric accuracy of AAA and CCC algorithms in the presence of eXaSkin bolus was assessed by gamma index. Generally, our findings demonstrated no significant differences between AAA and CCC algorithms and they could be used as alternatives in the presence of eXaSkin bolus. In addition, the eXaSkin bolus increased the surface dose about 25%; thus it is recommended for the radiotherapy of superficial lesions.

Acknowledgment

This article was extracted from a master's thesis in Medical Radiation Engineering by the first author at Islamic Azad University (Tehran, Iran). The authors would like to thank R. Abedi-Firouzjah for his helpful suggestions. The authors also would like to thank the Medical Physics team at the Radiotherapy and Oncology Department of Shohada-e-Tajrish Hospital for their sincere cooperation.

References

1. Ataei G, Rezaei M, Gorji KE, Banaei A, Goushbolagh NA, Farhood B, Bagheri M, Firouzjah RA. Evaluation of dose rate and photon energy dependence of gafchromic EBT3 film irradiating with 6 MV and Co-60 photon beams. Journal of medical signals and sensors. 2019 Jul;9(3):204.
2. Healy E, Anderson S, Cui J, Beckett L, Chen AM, Perks J, Stern R, Mayadev J. Skin dose effects of postmastectomy chest wall radiation therapy using brass mesh as an alternative to tissue equivalent bolus. Practical radiation oncology. 2013 Apr 1;3(2):e45-53.
3. Butson MJ, Cheung T, Yu P, Metcalfe P. Effects on skin dose from unwanted air gaps under bolus in photon beam radiotherapy. Radiation Measurements. 2000 Jun 1;32(3):201-4.
4. Richmond N. The accuracy of treatment planning system dose modelling in the presence of brass mesh bolus. Reports of practical oncology and radiotherapy. 2017;22(5):354-9.
5. Kourinou KM, Mazonakis M, Lyraraki E, Stratakis J, Damilakis J. Scattered dose to radiosensitive organs and associated risk for cancer development from head and neck radiotherapy in pediatric patients. Physica Medica. 2013 Nov 1;29(6):650-5.
6. Chandraraj V, Stathakis S, Manickam R, Esquivel C, Supe SS, Papanikolaou N. Comparison of four commercial devices for RapidArc and sliding window IMRT QA. Journal of applied clinical medical physics. 2011 Mar;12(2):338-49.
7. Bagheri H, Firouzjah RA, Farhood B. Measurement of the photon and thermal neutron doses of contralateral breast surface in breast cancer radiotherapy. Journal of Radiotherapy in Practice. 2020 Sep;19(3):226-32.
8. Jung H, Kum O, Han Y, Park B, Cheong KH. Photon beam dosimetry with EBT3 film in heterogeneous regions: Application to the evaluation of dose-calculation algorithms. Journal of the Korean Physical Society. 2014 Dec;65(11):1829-38.
9. Sim GS, Wong JH, Ng KH. The use of radiochromic EBT2 film for the quality assurance and dosimetric verification of 3D conformal radiotherapy using Microtek ScanMaker 9800XL flatbed scanner. Journal of applied clinical medical physics. 2013 Jul;14(4):85-95.
10. El Barouky J, Fournier-Bidoz N, Mazal A, Fares G, Rosenwald JC. Practical use of Gafchromic® EBT films in electron beams for in-phantom dose distribution measurements and monitor units verification. Physica Medica. 2011 Apr 1;27(2):81-8.
11. Massillon-JL G, Muñoz-Molina ID, Díaz-Aguirre P. Optimum absorbed dose versus energy response of gafchromic EBT2 and EBT3 films exposed to 20–160 kV x-rays and 60Co gamma. Biomedical Physics & Engineering Express. 2016 Jul 27;2(4):045005.
12. Abedi Firouzjah R, Nickfarjam A, Bakhshandeh M, Farhood B. The use of EBT3 film and Delta4 for the dosimetric verification of EclipseTM treatment planning system in a heterogeneous chest phantom: an IMRT technique. International Journal of Radiation Research. 2019;17(2):355-61.

13. Eduardo Villarreal-Barajas J, Khan RF. Energy response of EBT3 radiochromic films: implications for dosimetry in kilovoltage range. Journal of applied clinical medical physics. 2014 Jan;15(1):331-8.
14. Borca VC, Pasquino M, Russo G, Grosso P, Cante D, Sciacero P, Girelli G, Porta MR, Tofani S. Dosimetric characterization and use of GAFCHROMIC EBT3 film for IMRT dose verification. Journal of applied clinical medical physics. 2013 Mar;14(2):158-71.
15. Seidel MO, Miranda SV, Perea EM. Dosimetric characterization of exaskin: High density bolus for photon use. Reports of Practical Oncology & Radiotherapy. 2013(18):S355.
16. Ordonez-Sanz C, Bowles S, Hirst A, MacDougall ND. A single plan solution to chest wall radiotherapy with bolus?. The British journal of radiology. 2014 May;87(1037):20140035.
17. Zhen H, Hrycushko B, Lee H, Timmerman R, Pompoš A, Stojadinovic S, Foster R, Jiang SB, Solberg T, Gu X. Dosimetric comparison of Acuros XB with collapsed cone convolution/superposition and anisotropic analytic algorithm for stereotactic ablative radiotherapy of thoracic spinal metastases. Journal of applied clinical medical physics. 2015 Jul;16(4):181-92.
18. Niroomand-Rad A, Blackwell CR, Coursey BM, Gall KP, Galvin JM, McLaughlin WL, Meigooni AS, Nath R, Rodgers JE, Soares CG. Radiochromic film dosimetry: recommendations of AAPM radiation therapy committee task group 55. Medical physics. 1998 Nov;25(11):2093-115.
19. GAFChromic™ EBT3 film specifications, Available at www.gafchromic.com.
20. Arjomandy B, Tailor R, Anand A, Sahoo N, Gillin M, Prado K, Vicic M. Energy dependence and dose response of Gafchromic EBT2 film over a wide range of photon, electron, and proton beam energies. Medical physics. 2010 May;37(5):1942-7.
21. Devic S. Radiochromic film dosimetry: past, present, and future. Physica medica. 2011 Jul 1;27(3):122-34.
22. Low, D.A., et al., A technique for the quantitative evaluation of dose distributions. Medical physics, 1998. 25(5): p. 656-661.
23. Manger R, Paxton A, Cerviño L. Dosimetric assessment of brass mesh bolus for postmastectomy photon radiotherapy. Journal of applied clinical medical physics. 2016 Nov;17(6):86-96.
24. Hardcastle N, Basavatia A, Bayliss A, Tomé WA. High dose per fraction dosimetry of small fields with Gafchromic EBT2 film. Medical physics. 2011 Jul;38(7):4081-5.
25. Lárraga-Gutiérrez JM, García-Hernández D, García-Garduño OA, Galván de la Cruz OO, Ballesteros-Zebadúa P, Esparza-Moreno KP. Evaluation of the Gafchromic® EBT2 film for the dosimetry of radiosurgical beams. Medical physics. 2012 Oct;39(10):6111-7.
26. Hasenbalg F, Neuenschwander H, Mini R, Born EJ. Collapsed cone convolution and analytical anisotropic algorithm dose calculations compared to VMC++ Monte Carlo simulations in clinical cases. Physics in Medicine & Biology. 2007 May 24;52(13):3679.
27. Aarup LR, Nahum AE, Zacharatou C, Juhler-Nøttrup T, Knöös T, Nyström H, Specht L, Wieslander E, Korreman SS. The effect of different lung densities on the accuracy of various radiotherapy dose calculation methods: implications for tumour coverage. Radiotherapy and oncology. 2009 Jun 1;91(3):405-14.